Journal of
Materials Chemistry B

Materials for biology and medicine

Accepted Manuscript

This article can be cited before page numbers have been issued, to do this please use: P. Wang, C. Geng, L. Pan and B. Liu, *J. Mater. Chem. B*, 2020, DOI: 10.1039/C9TB02564B.

ROYAL SOCIETY OF CHEMISTRY

rsc.li/materials-b

Carbon Nanocoil Based Flexible Tip for Live Cell Study of Mechanotransduction and Electro-physiological Characteristics

Peng Wang[1,3+], Chunyang Geng[2+], Lujun Pan[1]*, Bo Liu[2]*

1 School of Physics, Dalian University of Technology, No.2 Linggong Road, Ganjingzi District, Dalian, Liaoning, 116024, P.R. China

2 Department of Biomedical Engineering, Dalian University of Technology, No.2 Linggong Road, Ganjingzi District, Dalian, Liaoning, 116024, P.R. China

3 Physics Department, Xinzhou Teachers University, No.10 Heping West Street, Xinzhou, Shanxi, 034000, P.R. China

[+]These authors contributed equally to this work.
*Corresponding Author Email address: lpan@dlut.edu.cn (L. Pan); lbo@dlut.edu.cn (B. Liu)

Abstract

The responses of living cells to external mechanical and electrical stimulation play important roles in regulating their biological functions and behaviors, and the response mechanisms have attracted great attentions. Global stimulation on cells is generally used in traditional methods, but it is insufficient to investigate the mechanism of dynamic physiological response at the subcellular level. At present, there is still lack of a low-cost and easy-operated method to apply local mechanical force and electrical stimulation to living cells. In this work, an individual carbon nanocoil (CNC) is used as a microscale noninvasive tool for local stimulation on single cell, and a living cell imaging technology, fluorescence resonance energy transfer (FRET), is adopted to determine the responses of cells. After demonstrating that CNCs have low cytotoxicity to be applied in biological field, an individual CNC is used as a needle tip to apply local mechanical force on a single osteosarcoma cell, which is transfected with a Src FRET biosensor to explore the mechano-physiological response. A spatial increasing and polarized Src protein activation is observed on the stimulated cell. Moreover, a single CNC is also used as an electrode to exert periodic local electrical stimulation. Osteosarcoma cells transfected with calcium-FRET biosensors show notable spatial polarized FRET emission ratio distribution, then the FRET ratio shows a recoverable tendency towards the initial state after withdrawing the electrical stimulation. The cell biofunctions and structures are not damaged during the experiment process, which indicates CNC is a kind of non-invasive and bio-safe tip. The CNC tip is a powerful tool for exploring the mechanotransduction and electro-physiological characteristics of living cells.

Keywords: Carbon nanocoil; fluorescence resonance energy transfer; local mechanical force; local electrical stimulation;

1. Introduction

The sensing and response of living cells to external mechanical and electrical stimulation are crucial for cellular behaviors and diseases [1-4]. Thus, the cellular mechanotransductions and electrophysiological characteristics have attracted great attentions, and many physical methods have been developed for investigating the underlying mechanisms.

For the study of cellular mechano-physiological characteristics, parallel-plate flow chamber is a traditional tool mimicking the vessel to apply global shear stress on cells for exploring the heterogeneous changes in cell function, such as polarized Src and FAK activation [5, 6]. However, parallel-plate flow chamber cannot exert local mechanical stimulation which hampers the study of transduction mechanism, many improved methods are developed. A matrix glue traction system is developed to applies local mechanical stimulation on a human umbilical vein endothelial cell [7]. Azeloglu et.al develops an atomic force microscope (AFM) elastography technique to map spatiotemporal stiffness of isolated, in which rat cardiomyocytes are indented repeatedly by the AFM probe [8]. Microbeads are also adopted for exerting local force on cells. Dao et.al develops a quantitative model for investigating the mechanical deformation characteristics of the red blood cell by means of optical tweezer-controlled-microbeads [9]. With magnetized microbeads, Feneberg et.al studies the local viscoelasticity of the apical membrane of human umbilical vein endothelial cells by magnetic tweezers microrheometry [10].

For the study of cellular electrophysiological characteristics, the patch clamp, which consists of a microtubule electrode and an amplifying circuit, is a popular and powerful tool. It shows the activity of the ion channel molecule on cell membrane by recording the ion current of the ion channel. In addition to this function, Hamilton et.al uses a glass micropipette filled with artificial cerebrospinal fluid to apply electrical stimulation on nerves, meanwhile, the sharp glass micropipette is mounted on a micromanipulator directly to apply a mechanical stimulation on astrocytes [11]. The cellular environment in vivo includes various signals such as mechanical and electrical signals, which jointly play a critical role in the regulation of differentiation, maturation, function and behavior of living cells such as cardiomyocyte [4]. Ossola et.al combines the patch clamp with AFM techniques. The novel AFM probe is able to apply mechanical force and electrical stimulation on single cells, and to obtain electrophysiological and mechanical signal simultaneously [12]. Pavesi et.al designs and fabricates a micro-scale cell stimulator. The stimulator performs stretching on the substrate to provide mechanical stimulation and applies a uniform electric field simultaneously to provide global electrical stimulation on cells [13]. Similarly, Miklas et.al describes a bioreactor for applying mechanical and electric field stimulation simultaneously on cardiomyocytes [14]. However, most of the methods mentioned have the

View Article Online
DOI: 10.1039/C9TB02564B

disadvantages of complex operation, high cost, low success rate and difficult analysis, there is still lack of a low-cost method to apply local mechanical and electrical stimulation on a single living cell. A new method with simple operation, non-damage and ability to exert local mechanical or electrical stimulation on cell is urgently needed.

Due to their inherent biocompatibility, remarkable physical and chemical properties, carbon nanomaterials are considered as appropriate candidates for biological applications [15-22]. Particularly, carbon nanotube (CNT) based cellular microprobe arrays [23-26], for the stimulation and detection of cellular mechano and electro-physiology, have gained considerable interests to solve the challenges mentioned above. However, the fabrication process of an elaborate and functional array is expensive and time-consuming. Moreover, because of the extremely tiny size, it is also difficult to manipulate a single CNT and graphene directly under an ordinary optical microscope, and furthermore to operate on an individual cell. As an emerging branch of carbon nanomaterials, carbon nanocoils (CNCs) are famous of their unique helical morphology, which have many advantages in biological fields, especially at cellular level. CNCs have large aspect ratio, with dozens of microns in length while smaller than 1 μm in coil diameter. Thus, CNCs are compatible to be manipulated handily under an ordinary optical microscope, and CNCs are lateral flexible to offer local mechanical stimulation on a single cell, in the scale of pico-Newton [27], accurately and noninvasively. What is more, due to their high electrical conductivity [28, 29], CNCs are good candidates as electrodes for cellular electrical stimulation and measurement. Thus, CNCs have great potential to be applied as bio-probes or bio-electrodes at cellular level. However, CNCs have not been used for biological applications to date.

In this paper, an individual CNC is used to apply local mechanical and electrical stimulation on osteosarcoma cells, and the responses of osteosarcoma cells are studied based on fluorescence resonance energy transfer (FRET) technology to prove its effectiveness. The CNC based flexible tip is demonstrated to be a new multifunctional tool for the investigation of mechanotransduction mechanism and electrophysiological characteristics of living cells.

2. Materials and methods

2.1. *Preparation of CNC-based tips*

CNCs have been synthesized by the pyrolysis of acetylene over an Fe-Sn-O catalyst through a thermal chemical vapor deposition (CVD) method [30]. $Fe_2(SO_4)_3 \cdot 9H_2O$ and $SnCl_2 \cdot 5H_2O$ were dissolved in distilled water as the catalyst precursor, and then the precursor was dropped on a quartz substrate and dried at 45 ℃ in air, followed by a calcination process at 710 ℃ in air for 0.5 h. The CNCs were synthesized on the sample at 710 ℃ for 2 h under the flow rate of acetylene and Ar gases of 15, 325

sccm, respectively. The prepared CNCs have unique helical morphologies, with an average coil diameter of 390 nm, an average fiber diameter of 230 nm, and an average pitch of 450 nm, respectively. A tungsten probe, which is fixed on a 3D micro manipulation, was used to contact the tip of a CNC protrudent from the as-grown CNCs, under an ordinary optical microscope. The single CNC and the tungsten tip were sticking together by silver paste, and then the single CNC was extracted out from the CVD-prepared CNC grass. A single CNC is shown in Figure 1. The insert is the TEM image of single CNC, which indicates CNC's unique helical morphology. Finally, the CNC was installed onto a 3D adjustable micromanipulator for further utilization.

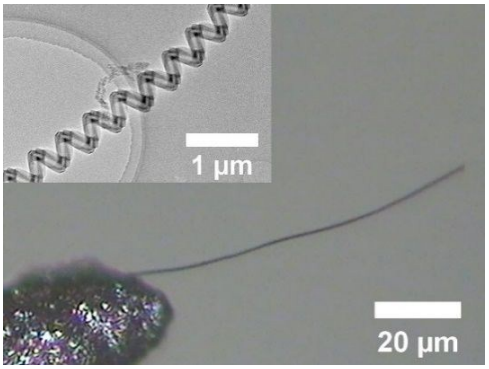

Figure 1. Optical image of a single CNC. The inset is the TEM image of CNC.

An electromechanical vibration method is used to measure the lateral stiffness of CNC [31]. A CNC is stimulated to vibrate under an alternating electric field. A curve between the amplitude and the frequency of vibration of the CNC is measured and is used to determine the CNC's resonance frequency (f), then the lateral stiffness (k) of CNC is calculated as below

$$k = 3\rho V(\frac{2\pi f}{1.875^2})^2, \quad (1)$$

where ρ and V are the density and volume of the CNC. The lateral stiffness is used to determine the force applied on a single cell, with the deflection of CNC. The k value is not a constant while varies with the size (such as length and coil diameter) of CNC, thus each CNC tip is measured separately before the mechanical stimulation experiment. In general, the CNCs used in our experiments are almost 50 μm in length, the lateral stiffnesses of them are measured to be in a scale of (5.2 ± 2.7) × 10^{-5} N/m (52 ± 27 pN/μm).

2.2. *Culturing of cells*

The human osteosarcoma cell line (U-20 S) was purchased from the Cell Bank of the Chinese Academy of Sciences (Shanghai, China). A sterile cell culture dish, which contained 2 mL of culture

View Article Online
DOI: 10.1039/C9TB02364B

medium, was used to culture cells in a 5% CO_2 incubator at 37 °C. Culture medium contained 89% RPMI Medium Modified (HyClone, USA), 10% fetal bovine serum (FBS) (Sigma-Aldrich, USA) and 1% Penicillin/Streptomycin solution (PS) (Gibco, USA).

2.3. *Biocompatibility characterization*

To explore the biocompatibility of CNC, cell proliferation was assessed using 3- (4, 5-dimethyl-2-thiazolyl) -2, 5-diphenyl-2-H-tetrazolium bromide (MTT) assay (Solarbio, USA). Cells were seeded into 96-well plates and divided into two groups. One group of cells was co-cultured with CNCs, and the other group was kept as control. After 24 h, 20 μl of 5 mg/mL MTT was added into each well and incubated for 4 h in the incubator. After discarding the supernatant, 200 μL of DMSO was added to each well to dissolve the formazan. The optical density (OD value) was measured at 490 nm by the microplate reader (Bio-Rad, USA) [32].

2.4. *Transfection of FRET biosensors:*

The fluorescence pairs were adopted as enhanced cyan fluorescent proteins (ECFP) and enhanced yellow fluorescent proteins (EYFP), where ECFP was fluorescence donor while EYFP was accepter. The CNC-induced mechanical response was examined with a membrane-bound FRET biosensor (Lyn-FAK) [6]. The mechanical stimulation induced the FAK activation to change the distance between the fluorescent donor and acceptor, then the variation of FRET efficiency was observed. Similarly, the CNC-induced electrical response was determined with a FRET-based Ca^{2+} biosensor [33]. The electrical stimulation opened the ion channels and allowed calcium ions to enter cells, then the FRET-based Ca^{2+} biosensor was activated and notable FRET variation was observed. The above FRET biosensors were transfected into cells using Lipofectamine 3000 (Invitrogen, USA). The optical image of U-20 S cells and relating fluorescence images of the ECFP and EYFP are shown in Supporting Information Figure S1. The peak wavelengths of the excited laser, donor emission light and accepter emission light were 440 nm, 480 nm and 535 nm, respectively.

2.5. *Microscopy and image analysis*

Before imaging experiments, recombinant plasmids of fluorescent biosensors were transfected into cells. Then, the proteins of fluorescent biosensors, named exogenous proteins, were expressed in cells. Thus, the cells were marked with fluorescent biosensors and cultured for 24 ~ 48 h. All images were taken by using an inverted microscope (Olympus IX73, Tokyo, Japan) equipped with a cooled charge coupled device. The Cellsense software was used with an excitation filter (440DF20), a dichroic

mirror (455DRLP) and two emission filters controlled via a filter controller, i.e. 480DF30 for ECFP and 535DF25 for EYFP. Before applying the stimulation, five images, with 1 min of interval between every two images were taken to determine the FRET baseline of the cells without stimulation. In order to detect the FRET response of the cells under mechanical stimulation, 30 images with the same interval were taken during the stretch application. While for electrical stimulation, 8 images were taken during the electrical stimulation, another 8 images were taken after ending the stimulation, with the interval of 7 s between every two images. The obtained images were processed after subtracting the fluorescence noise background to get the FRET emission ratio variation of the activated cell, by MATLAB software (MathWorks, USA). The fluorescence imaging procedure is shown in Figure S5 in Supporting Information.

2.6. *Statistical analysis*

Through MATLAB software, all the ratio data were normalized by their basal levels before stimulation in the same cell. Comparison between two groups was conducted using two-tail t-test and difference was considered to be statistically significant when the *P* value was less than 0.05.

3. Results

U-20 S cells are co-cultured with CNCs in order to explore the biocompatibility of CNCs. The optical density (OD value) of the MTT assay is used to show the cell viability. Figure 2a and 2b shows the optical images of the non-CNC group cells and the CNC-cultured group cells, respectively. As shown in Figure 2c, the viability of co-cultured group cells has no significantly difference with the control group, which indicates that CNCs have little side effect on the survival of living cells, namely CNCs have excellent biocompatibility.

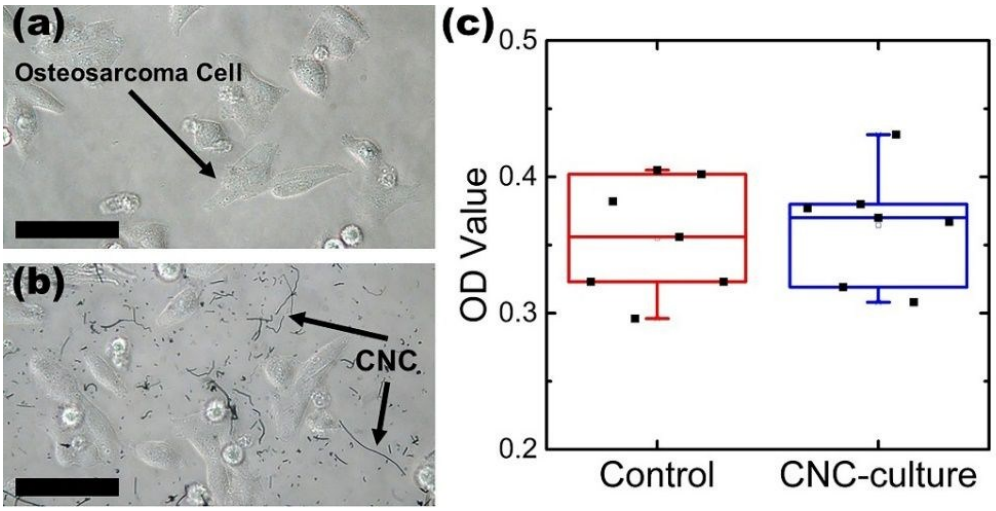

Figure 2. The optical images of U-20 S cells in (a) control group and (b) CNC-cultured group. The concentration of CNCs is 40 ppm. The scale bar is 50 μm. (c) The optical density of MTT assay for cell viability.

In order to explore the mechano-physiological response of a single cell, an individual CNC is fixed on a 3D micromanipulator to apply local mechanical stimulation. Figure 3a shows the local mechanical stimulation on a cell, and the force direction is indicated by the arrow. The dynamic process is shown in Movie S1 in Supporting Information. The applied force from CNC tip is described as

$$F_{\mathrm{CNC}} = k \times \Delta s\,, \tag{2}$$

where F_{CNC} is the applied force from CNC. Δs is the lateral deformation of the CNC after exerting force on cells, which is determined by the 3D micromanipulator directly. The manipulator is shown in Figure S2. k is the lateral stiffness of CNC, which was measured by electromechanical vibration method [31]. The CNCs used in our experiments are almost 50 μm in length, the lateral stiffnesses of them are measured to be in a scale of 5×10^{-5} N/m. Since the deflection of the CNC is several to ten micrometers, the mechanical force of the CNC is hundreds of pico-newtons, in general. During the mechanical experiment, the CNC is kept stable in order to exert a constant force rather than a varied force on a cell. The lower panel of Figure 3a shows the spatial FRET efficiency distribution of the cell under an invariant local stimulation of CNC. Due to the tiny contact area between the CNC and the cell, the FRET response appears in a polarized manner. The FRET efficiency of the area contacted with the CNC tip shows a more obvious and fast increment compared to other areas on the cell, and the spatial polarized distribution mainly appears in the first ten minutes of the stimulation. Dao et.al stretched the cell membrane with optical tweezers, and found that the cell deforms obviously under the mechanical force in the range of dozens to hundreds of pico-Newtons [9]. In our study, the magnitude of the force from CNC is calculated to be several hundreds of pico-Newtons. The stimulated cells under local mechanical stimulation show local deformations as those under the manipulation of optical tweezers, that's why the cells show spatial polarized FRET responses at first 10 minutes. Liu et. al have demonstrated that the membrane fluidity plays an important role in the biosensors' activation in response to shear stress [6]. Thus, it is considered that the disappear of the polarized FRET activation after 10 min comes from the membrane fluidity, which leads to a new uniform equilibrium state of the cell membrane, namely the stimulated cell maintains the uniform state in response to the external force globally, rather than locally. Figure 3b shows the relationship between the CNC-induced average FRET efficiency and time for U-20 S cells. The average FRET efficiency of the cell increases gradually with applying the mechanical stimulation continuously.

View Article Online
DOI: 10.1039/C9TB02564B

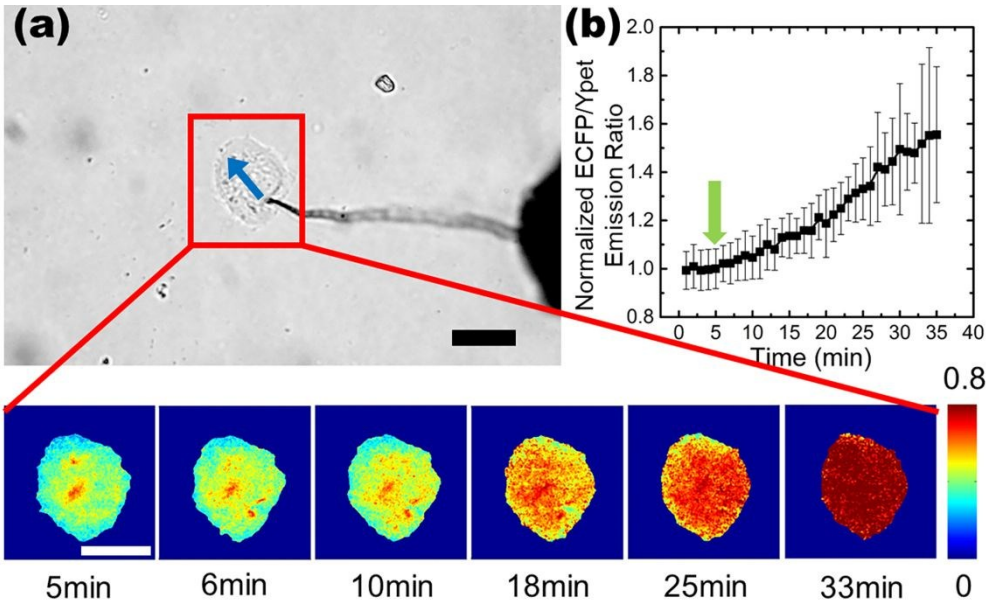

Figure 3 Effect of mechanical stimulation on U-20 S cells (*n*=7). Five images were taken before applying the stimulation to determine the FRET baseline of the cells without stimulation, and thirty images were taken during the stretch application, the interval between every two images is 1 min. The obtained images were processed after subtracting the fluorescence noise background to get the FRET emission ratio variation of the activated cell. (a) The upper panel shows the optical image of a single CNC is stimulating on an osteosarcoma cell mechanically. The lower panel shows the distribution of the FRET emission ratio at different times. (b) The statistical results of the FRET emission ratio with time for the mechanically stimulated osteosarcoma cells. The green arrow indicates the beginning of the mechanical stimulation. The scale bar is 10 μm.

When cells are electrically stimulated, some calcium channels on cell membrane are opened with the alternation of membrane potential. A large number of calcium ions in the culture medium pour into the cell, which results in the enhancement of FRET emission ratio which could show the responses of the cells to electrical stimulation. Hence, an individual CNC is also fabricated as a microscale electrode to characterize the electrophysiology of osteosarcoma cells. In order to eliminate the influences of mechanical actions and enhance the local effects, the CNC electrode is in point contact with the cell membrane softly, as shown in Figure 4a. The CNC tip is connected to the negative electrode of a signal generator to exert electrical stimulation on a single cell, while a platinum electrode is grounded as a counter electrode to clamp the solution potential. A periodic negative voltage of -100 mV with a width of 100 ms per 7 s was applied to a single osteosarcoma cell, through the CNC-based electrode. The electrical signal of CNC was recorded by an oscilloscope, as shown in Supporting Information Figure

S3. In order to reveal the response characteristics to the electrical stimulation, the osteosarcoma cells are transfected with FRET-based Ca^{2+} biosensor.

As the circuit switching on, the FRET photos begin to be taken. As shown in lower panel of Figure 4a, the FRET efficiency of the activated cell exhibits remarkable polarized distribution. The FRET efficiency increases preferentially at the contact side between the CNC and the cell, and diffuses towards to the other side gradually. The FRET ratio distribution becomes uniform eventually, and shows a recoverable tendency towards the initial state after withdrawing the stimulation. Obviously, the FRET ratio polarized distribution comes from the local electrical stimulation of the CNC electrode. Figure 4b shows the temporal FRET emission ratio curve of osteosarcoma cells before (0~28 s), under (28~77 s) and after (77~140 s) the electrical stimulation. It is found that the average FRET efficiency shows a significant and rapid increment when cells are electrically stimulated by CNC electrode, and the FRET ratio decreases gradually after removing the CNC.

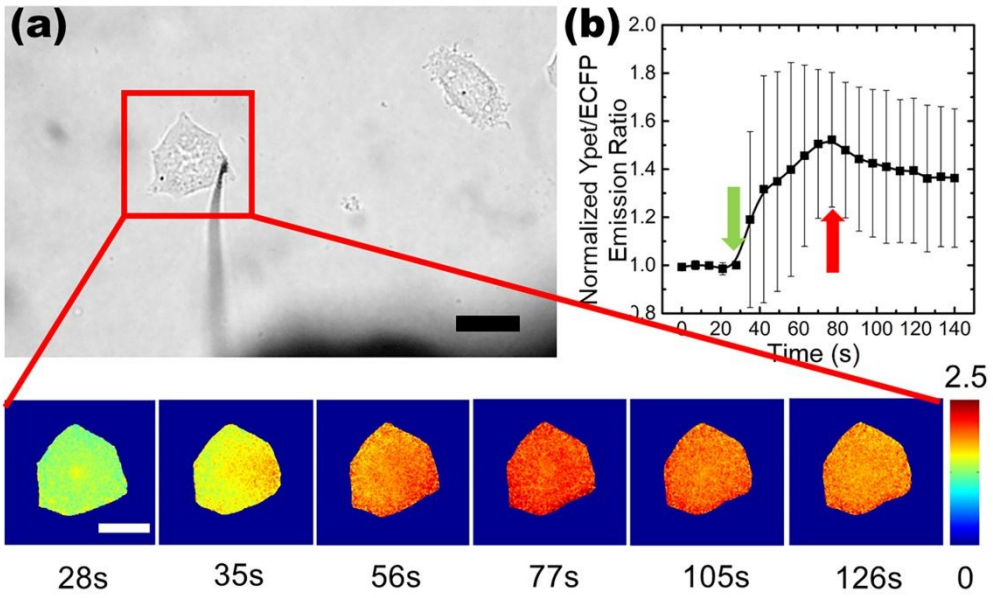

Figure 4 Effect of electrical stimulation on U-20S cells (n=5). Five images were taken before applying the stimulation to determine the FRET baseline of the cells without stimulation, and eight images were taken during the electrical stimulation, another eight images were taken after ending the stimulation, the interval between every two images is 7 s. The obtained images were processed after subtracting the fluorescence noise background to get the FRET emission ratio variation of the activated cell. (a) The upper panel shows the optical image of a single CNC stimulating electrically on an osteosarcoma cell. The lower panel shows the typical representative FRET ratio images at different times. Remarkable spatial polarized FRET ratio shows the polarized responses of the cell under the local electrical stimulation. (b) The statistical time course of the FRET emission ratio for

the electrically stimulated osteosarcoma cells. The green arrow indicates the beginning of the electrical stimulation while the red arrow indicates the end. The scale bar is 10 μm.

4. Discussion

Compared to the control group, osteosarcoma cells co-cultured with CNCs grow well, which indicates the good biocompatibility of CNCs. Combined with FRET technology, the CNC-based needle tip is used for the investigation of living cell mechanotransduction and electrophysiological characteristics for the first time. When a single CNC is used to apply local mechanical force quantitatively on osteosarcoma cells, the FRET efficiency of living cells shows a notable variation increment and spatial polarized response. While the CNC is adopted as a bio-electrode for local electrical stimulation on living cells, the FRET efficiency of living cells shows obvious polarized manner and a recoverable tendency towards the initial state after removing the CNC. The remarkable polarized changes of the FRET efficiency in cells under mechanical or electrical stimulation are similar to the results of other methods, such as the parallel-plate flow chamber and drugs [6, 11]. The results above show that the CNC-based needle tips could exert enough local mechanical and electrical stimulation on cells.

As shown in Fig. 3a, the FRET efficiency of the area contacted with the CNC shows a more notable increment compared to other areas of the cell. Therefore, spatiotemporal change in the FRET response is correlated with the location of the applied force. Wang et.al utilized the laser-tweezer traction in the study of mechano-activation of Src. The results showed that the FRET responses of a cell with clear directional wave propagation were away from the site of mechanical stimulation [34]. The CNC is an efficient tool which is more easily to operate than the laser-tweezer, it could be used for investigating the relationship between the spatiotemporal change of the FRET response and the direction of the applied force. For more accurate measurement of the mechanical force, using CNCs with force sensing capability is a subject for the future study.

Compared to other methods, the CNC has a lot of advantages. A single CNC tip is able to apply local mechanical or electrical stimulations on a single cell, which is superior to the parallel-plate flow chamber, the micro-scale cell stimulator and bioreactor for overcoming the limitation of applying the stimulation globally [5, 13, 14]. In addition, as shown Fig. S4, the CNC has a blunt rather than sharp tip, thus the CNC keeps contact with the target cell non-invasively, while not pierce into the cell. The CNC can be easily removed from the cell, which is proven by the Movie S1 in Supporting Information. After the mechanical or electrical stimulation, the cells didn't show notable deformations, as shown in the fluorescent images of cells (Figure 3 and 4). In addition, after removing the CNC electrode, calcium

ions are excluded from the cell, which results in the decrease of FRET efficiency. Thus, the physiological function of activated cells is not damaged during the experiment. Above results show that the cells kept good activity. If not, the cells will separate from the substrate and become round. Therefore, CNCs are considered to be non-invasive and safe. Moreover, the CNC tip is operated under an ordinary optical microscope to apply mechanical and electrical stimulation on cells without any expensive machine such as AFM, which reduces the cost of experiment operation [8, 12]. This method is easier than handling the beads attached to cell membrane by means of optical tweezers or magnetic field [9, 10], while CNC is easy to operate through a 3D micromanipulation, which reduces the difficulties of experimental operation and quantitative calculation of the applied force. Meanwhile, CNCs have good mechanical property, which simplifies the calculation of the mechanical force applied on cells, instead of the complex computer models and physical laws for the laser tweezer or magnetic field using beads [35]. What's more, CNCs have very good conductivity; it is possible to use a CNC as an electrode to apply electrical stimulation on cells. Compared to the micropipette of patch clamp, the CNC-based needle tip with an invariable conductivity doesn't need to additional electrolyte, which may cause unstable resistance and further result in inconstant electrical stimulation [12, 36]. For more accurate of electrical stimulation on cell, the encapsulation for CNC electrode with an insulating layer is the next research topic. CNCs also show the advantage of good biocompatibility.

The large variation in the FRET emission ratio shown in Figure 4b comes from the large fluctuation of the concentration of calcium ions, which is a universal phenomenon in the current study. Tuchiya et.al demonstrates that the average concentration of the cytosolic calcium from 54.1 ± 2.0 nM to 350.5 ± 85.9 nM in response to 10^{-5} M noradrenaline [37]. In addition, the analysis of the spatiotemporal FRET emission ratio distribution under multiple stimulations is more complex than that under single stimulation. We have already begun to develop a new method based on clustering analysis and neural network algorithm, for the further quantitative analysis of the spatiotemporal distribution.

5. Conclusion

Combined with FRET technology, CNC-based needle tips are used for the investigations of living cell local mechanical transduction and electrophysiological characteristics for the first time. It is demonstrated that CNCs have excellent biocompatibility to be applied in biological fields. The instinct biocompatibility, tiny size, excellent mechanical and electrical properties of CNCs benefit them to study the irritabilities of living cells, as non-invasive tips. A single CNC is used to exert local mechanical force quantitatively on osteosarcoma cells. The FRET emission ratio of living cells shows

obvious increment under the CNC-stimulation, and shows spatial polarized response to some extent. The individual CNC is also adopted as a bio-electrode for local electrical stimulation on living cells. The FRET ratio of living cells shows obvious polarized manner, and returns to the initial state after removing the CNC tip. Thus, CNCs are powerful, universal and user-friendly tools for the investigations for intracellular mechanical and electrical transduction mechanism, cellular behaviors regulation and cellular electrical signal detection.

Acknowledgements

This work was supported by the National Natural Science Foundation of China (Nos. 51661145025, 11274055, 31670867).

References

1. M. I. Papafaklis, S. Takahashi, A. P. Antoniadis, A. U. Coskun, M. Tsuda, S. Mizuno, I. Andreou, S. Nakamura, Y. Makita, A. Hirohata, S. Saito, C. L. Feldman and P. H. Stone, *Atherosclerosis*, 2015, **240**, 205-211.
2. T. Morimoto, T. Miyoshi, T. Fujikado, Y. Tano and Y. Fukuda, *Neuroreport*, 2002, **13**, 227-230.
3. G. Eng, B. W. Lee, L. Protas, M. Gagliardi, K. Brown, R. S. Kass, G. Keller, R. B. Robinson and G. Vunjak-Novakovic, *Nat Commun*, 2016, **7**, 1-10.
4. W. L. Stoppel, D. L. Kaplan and L. D. Black, *Adv Drug Deliver Rev*, 2016, **96**, 135-155.
5. J. G. McGarry, J. Klein-Nulend, M. G. Mullender and P. J. Prendergast, *Faseb J*, 2004, **18**, 482-484.
6. B. Liu, S. Y. Lu, Y. L. Hu, X. L. Liao, M. X. Ouyang and Y. X. Wang, *Sci Rep-Uk*, 2014, **4**, 1-8.
7. W. S. Nishitani, T. A. Saif and Y. X. Wang, *Plos One*, 2011, **6**, 1-8.
8. E. U. Azeloglu and K. D. Costa, *Am J Physiol-Heart C*, 2010, **298**, H853-H860.
9. M. Dao, C. T. Lim and S. Suresh, *J Mech Phys Solids*, 2003, **51**, 2259-2280.
10. W. Feneberg, M. Aepfelbacher and E. Sackmann, *Biophys J*, 2004, **87**, 1338-1350.
11. N. Hamilton, S. Vayro, F. Kirchhoff, A. Verkhratsky, J. Robbins, D. C. Gorecki and A. M. Butt, *Glia*, 2008, **56**, 734-749.
12. D. Ossola, M. Y. Amarouch, P. Behr, J. Voros, H. Abriel and T. Zambelli, *Nano Lett*, 2015, **15**, 1743-1750.
13. A. Pavesi, G. Adriani, M. Rasponi, I. K. Zervantonakis, G. B. Fiore and R. D. Kamm, *Sci Rep-Uk*, 2015, **5**, 1-12.
14. J. W. Miklas, S. S. Nunes, A. Sofla, L. A. Reis, A. Pahnke, Y. Xiao, C. Laschinger and M. Radisic, *Biofabrication*, 2014, **6**, 024113 024111-024114.
15. G. T. Feliciano, C. Sanz-Navarro, M. D. Coutinho-Neto, P. Ordejon, R. H. Scheicher and A. R. Rocha, *Phys Rev Appl*, 2015, **3**, 034003 034001-034007.
16. Q. Q. Tian, Y. Wang, R. J. Deng, L. Lin, Y. Liu and J. H. Li, *Nanoscale*, 2015, **7**, 987-993.
17. J. T. Robinson, S. M. Tabakman, Y. Y. Liang, H. L. Wang, H. S. Casalongue, D. Vinh and H. J. Dai, *J Am Chem Soc*, 2011, **133**, 6825-6831.
18. L. J. Meng, W. J. Xia, L. Liu, L. Y. Niu and Q. H. Lu, *Acs Applied Materials & Interfaces*, 2014, **6**, 4989-4996.
19. L. V. Nair, Y. Nagaoka, T. Maekawa, D. Sakthikumar and R. S. Jayasree, *Small*, 2014, **10**, 2771-2775.
20. M. Zhang, W. T. Wang, F. Wu, P. Yuan, C. Chi and N. L. Zhou, *Carbon*, 2017, **123**, 70-83.

View Article Online
DOI: 10.1039/C9TB02564B

21. B. R. Smith and S. S. Gambhir, *Chem Rev*, 2017, **117**, 901-986.
22. R. D. Mehlenbacher, R. Kolbl, A. Lay and J. A. Dionne, *Nat Rev Mater*, 2018, **3**, 17080 17081-17017.
23. J. Cools, D. Copic, Z. X. Luo, G. Callewaert, D. Braeken and M. De Volder, *Adv Funct Mater*, 2017, **27**, 1701083 1701081-1701089.
24. X. Zhang, S. Prasad, S. Niyogi, A. Morgan, M. Ozkan and C. S. Ozkan, *Sensor Actuat B-Chem*, 2005, **106**, 843-850.
25. M. J. Roberts, M. K. Leach, M. Bedewy, E. R. Meshot, D. Copic, J. M. Corey and A. J. Hart, *J Neural Eng*, 2014, **11**.
26. A. Beduer, F. Seichepine, E. Flahaut, I. Loubinoux, L. Vaysse and C. Vieu, *Langmuir*, 2012, **28**, 17363-17371.
27. P. Wang, L. J. Pan, C. W. Li and J. Zheng, *Nano*, 2018, **13**, 1850112 1850111-1850116.
28. H. Ma, K. Nakata, L. J. Pan, K. Hirahara and Y. Nakayama, *Carbon*, 2014, **73**, 71-77.
29. Y. M. Sun, C. W. Wang, L. J. Pan, X. Fu, P. H. Yin and H. L. Zou, *Carbon*, 2016, **98**, 285-290.
30. R. X. Cui, L. J. Pan, H. Ma, P. Wang and M. Asif, *Rsc Adv*, 2016, **6**, 30125-30129.
31. C. H. Deng, L. J. Pan, H. Ma and R. X. Cui, *Carbon*, 2015, **81**, 758-766.
32. S. L. Li, Y. Huang, Y. Huang, Y. M. Fu, D. L. Tang, R. Kang, R. R. Zhou and X. G. Fan, *J Exp Clin Canc Res*, 2017, **36**, 1-12.
33. B. Liu, S. Y. Lu, S. A. Zheng, Z. L. Jiang and Y. X. Wang, *Cardiovasc Res*, 2011, **91**, 124-133.
34. Y. X. Wang, E. L. Botvinick, Y. H. Zhao, M. W. Berns, S. Usami, R. Y. Tsien and S. Chien, *Nature*, 2005, **434**, 1040-1045.
35. E. L. Botvinick and Y. X. Wang, *Method Cell Biol*, 2007, **82**, 497-523.
36. K. L. Perkins, *J Neurosci Meth*, 2006, **154**, 1-18.
37. K. Tuchiya and M. Nagai, *Biomed Res-Tokyo*, 1994, **15**, 347-355.